Austin Journal of Biomedical Engineering

Austin Publishing Group

Open Access Full Text Article

Research Article

Cost-Efficient and Multi-Functional Systems for Ultrasound Measurement and Imaging

Jayanth Kandukuri[1,2], Yuan Liu[1,2] and Baohong Yuan[1,2]*

[1]Department of Bioengineering, University of Texas at Arlington, USA

[2]Joint Biomedical Engineering Program, The University of Texas at Arlington and the University of Texas Southwestern Medical Center at Dallas, USA

***Corresponding author:** Baohong Yuan, Bioengineering Department, University of Texas at Arlington, 500 UTA BLVD, Arlington, TX 76010, USA, Email: baohong@uta.edu

Received: January 20, 2014; **Accepted:** February 24, 2014; **Published:** March 05, 2014

Abstract

Two cost-efficient systems were designed and demonstrated for reconstructing ultrasound wave propagation and interference and for understanding the principles of ultrasound imaging and micro bubble-enhanced ultrasound imaging. One of the systems was based on a needle hydrophone that was mechanically scanned in an ultrasound focal zone, and the other system was based on a metal wire or needle, with a small diameter, that was translated in an ultrasound focal zone. The advantages and disadvantages of both methods were discussed. These systems are useful for students, educators, and researchers for investigating ultrasound wave properties and understanding ultrasound imaging principles when the budget is limited.

Keywords: Ultrasound; Pressure waves; Interference; Hydrophone; Imaging; Micro bubbles.

Introduction

An ultrasound wave represents a mechanical pressure wave that propagates in a medium. The behavior of an ultrasound wave has been well studied [1-4]. It can be well focused using an acoustic lens or a curved transducer. Also, it can be reflected and scattered due to acoustic impendence mismatching between the different media in which it propagates. Importantly, a short ultrasound pulse can be used to image noninvasively the acoustic impedance mismatch between two media based on a pulse-echo technique [1-2]. More interestingly, a high frequency ultrasound wave (in MHz range) can resonate with a micro bubble to generate a linear or a nonlinear acoustic signal for the enhancement of ultrasound imaging [1]. Micro bubbles are commonly used as ultrasound imaging contrast agents and are very tiny bubbles with a gas core shelled with a lipid, protein, or polymer layer [5-9]. Generally, they are smaller than ten microns in diameter, and the average size is around 2-3 microns to be able to pass tissue capillaries. They are usually used to enhance tissue ultrasound imaging, such as tissue perfusion imaging, blood flow imaging, molecular imaging, and drug delivery [1]. Therefore, developing a simple, cost-efficient, and multi-functional system for demonstrating these unique features of ultrasound physics and techniques is significantly useful for students, scientific educators, clinical professionals, and even members of the general public who are either interested in ultrasound but have limited ultrasound knowledge or who are newly entering the field. It is also a valuable tool for scientific researchers who are looking for a tool to quantify the static or dynamic properties of an ultrasound pressure field but have a limited budget.

Several techniques have been widely developed to measure ultrasound intensity distribution in media [2,10-12]. One of them is the Schlieren technique, which is based on the phenomenon of light diffraction by ultrasound waves in a transparent medium [10]. Ultrasound intensity is reconstructed based on the detected optical signals. Therefore, it is much faster than mechanical methods that involve mechanical scanning [2,11,12]. A few commercial systems have adopted the Schlieren technique, such as the OptiSon® ultrasound beam analyzer (from Onda, Inc.) [13]. Unfortunately, these systems are extremely expensive (>$150K), so they are most likely to be used by ultrasound transducer manufacturers to characterize their products. In addition, what this technique measures is the static or dynamic distribution of ultrasound **intensity**, instead of **pressure**. One may think that the intensity is related to the square of pressure. Therefore, if one can measure the pressure distribution, the intensity distribution can be calculated. However, the converse is not true, which means that pressure distribution cannot be extracted based on the measured intensity distribution because an ultrasound pressure field includes more information (both amplitude and phase) than an ultrasound intensity field, which contains only amplitude information. Therefore, other techniques have to be adopted to measure the dynamic propagation of an ultrasound pressure wave. A needle-shaped hydrophone or a fine wire, with diameter in range of hundreds of microns, can be used to measure ultrasound pressure wave [2,11,12]. While a needle hydrophone can directly measure the local pressure variation, a fine wire can function as a reflection target to generate an ultrasound echo that indirectly represents the local ultrasound pressure [2,11,12]. Therefore, the reflected ultrasound signal from the wire should be processed by considering the round trip echoes to observe correctly the local pressure variation (see Sections 2 and 3). There are many applications that require characterizing an ultrasound pressure field instead of an intensity field alone. For example, when we try to investigate how an interfered ultrasound wave affects the dynamic oscillation of an immobilized micro bubble, we would like to know how the ultrasound pressure distributes in the bubble area. Therefore, the reconstruction of an ultrasound pressure field is highly desirable not only for education, but also for research.

There may be some commercially available systems that can be used for the 2- or 3-dimentional reconstruction of an ultrasound pressure field based on a needle-shaped hydrophone (such as the AIMS system from Onda, Inc.) [14]. However, they are usually very

Citation: Kandukuri J, Liu Y , Yuan B. Cost-Efficient and Multi-Functional Systems for Ultrasound Measurement and Imaging. Austin J Biomed Eng. 2014;1(1): 1001.

expensive and are unaffordable for many educators, professionals, and researchers (including those researchers whose main research streams are not ultrasound but who need to measure a dynamic pressure field for some reason). Therefore, in this study, we developed a cost-efficient and multi-functional ultrasonic system that can be used to reconstruct the 2- or 3-dimentional dynamic variation of ultrasound pressure waves based on either a needle-shaped hydrophone or a small diameter wire. In addition, this system can be used to conduct ultrasound imaging and study micro bubble-enhanced ultrasound imaging. Although the principle of the developed system is straightforward, engineering challenges exist in the development of both hardware and software. Therefore, we would like to share our design, experience, and results to the community to make the system affordable.

This study is organized as follows. First, the principle of the system is introduced in section 2, including both hardware and software. Following that, several experiments, data processing, and results are demonstrated in section 3, including: (1) the reconstruction of a dynamic pressure field generated from focused 1, 2.25 and 5 MHz ultrasound transducer using a needle-shaped hydrophone; (2) the reconstruction of a dynamic pressure field generated from focused 1, 2.25 and 5 MHz ultrasound transducer using a small diameter wire or needle; (3) the reconstruction of a dynamic interfered pressure field generated from two unfocused 2.25 MHz ultrasound transducers using a needle-shaped hydrophone; and (4) single-element ultrasound imaging and micro bubble-enhanced ultrasound imaging using a focused 5MHz ultrasound transducer. We conclude this study in section 4.

System Design

Hardware

Ultrasonic pressure measurement system I—A needle-shaped hydrophone method:

If we assume that the velocity of an ultrasound pulse propagating in water is 1.48 mm/μs, it takes tens of microseconds to travel tens of millimeters. This is usually too fast to image the pressure dynamic distribution in 2- or 3-dimentional space. Therefore, our design idea is to reconstruct the dynamic propagation of an ultrasound pulse by measuring multiple identical (assumed) ultrasound pulses at different locations and time points. After measuring all of the necessary data, one can reconstruct the dynamic propagation of an ultrasound pulse in a 2- or 3-dimentional space by appropriately organizing and displaying the data. Thus, at the expense of data acquisition time, the system cost can be significantly reduced.

Figure 1 shows a schematic diagram of the measurement system. This system consists of three sub-systems: (1) ultrasound source; (2) data acquisition; and (3) mechanical translation. Each sub-system is highlighted by a dashed rectangle in Figure 1, and the shaded rectangle represents a water tank in which the ultrasound transducer and the hydrophone are submerged. In the ultrasound source section, an ultrasound transducer (UST) was driven by the sinusoidal burst signal generated by a function generator (FG, AFG 3252, Tektronix, TX, USA) to produce an ultrasound pressure pulse. In the data acquisition section, the ultrasound pressure pulse was detected by a needle-shaped hydrophone (HNP-0200, Onda Corporation, CA and USA). The hydrophone converted the ultrasonic pressure signal into an electronic signal that was further amplified by a broadband amplifier (AH-2010, Onda Corporation, CA and USA). The electronic voltage signal was then digitized by a broadband digitizer (USB 5133, National Instrument, TX and USA) and further acquired by a computer via custom-made software that was programmed using MATLAB. When the FG sends an electronic signal to excite the UST, it also sends out a synchronized voltage signal that is used to trigger the digitizer. Therefore, data acquisition is well synchronized with the excitation of the ultrasound pulse. In the mechanical translation section, a motorized 3-dimentional translation stage system (x-y-z, VXM motor driven X-Slide assemblies, Velmex, NY and USA) was adopted to shift the hydrophone to different locations. To avoid the motion artifact caused by the mechanical movement (order of milliseconds), an important design requirement is to well control the time delay between the data acquisition and the system scanning.

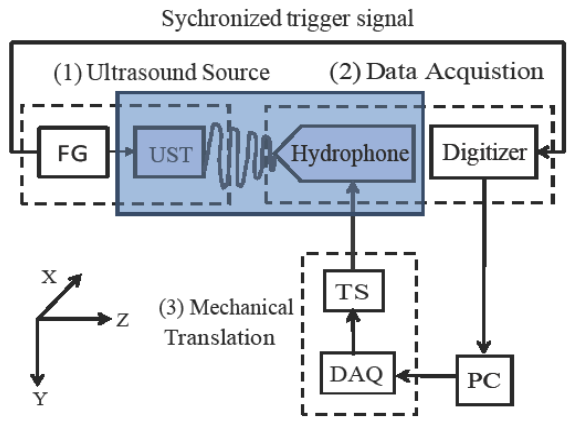

Figure 1: Block diagram of the experimental setup for imaging ultrasound propagation using a needle-shaped hydrophone. FG: function generator; UST: ultrasound transducer; TS: translation stage; DAQ: data acquisition card.

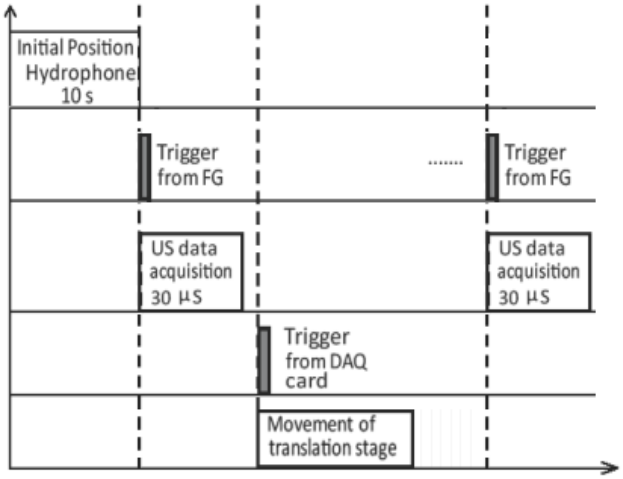

Figure 2: Time sequence of the operation for the entire system.

One of the shortcomings of the relatively low cost of the translation stage is the inability to provide a feedback signal to indicate the actual location. Thus, it cannot be used as a master clock to trigger the entire system. Therefore, an additional DAQ card (PCIe-6353, National Instrument, TX and USA) has been adopted to generate a digital voltage signal to trigger this scanning system (serving as a slave system). An adequate time interval (order of microseconds) between two succeeding triggers provided by the DAQ should allow the hydrophone to arrive at the desired location before data acquisition. To measure the wave propagation at the focal zone, the hydrophone is positioned around this focal area by detecting the location where the ultrasound signal is observed to be the maximum. Generally, a 10-second delay before the initiation of a raster scan is adopted in order to allow sufficient time for the hydrophone to be positioned at the desired location. The overall scanning duration depends upon the time taken to move between any two adjacent scan points which is limited by mechanical translations, desired resolution, number of times signal is average at each scan point for desired SNR, and the total number of scan points in scanning area. To be specific, if this system is used for 1 MHz ultrasound transducer, a scan of a 7.62 x 7.62 mm^2 image with a resolution of 0.2 x 0.25 mm^2 will take approximately 60 to 90 minutes depending upon the averaging at each scan point. This procedure is controlled by the custom developed MATLAB GUI software.

The time sequence of the operation of the entire system is displayed in Figure 2. Initially, the hydrophone is positioned in the focal area of the UST where the ultrasound pressure reaches the maximum and this location is considered as the center of the focal zone. The digitizer starts accepting the trigger signals from the FG, which is controlled by the MATLAB software. Because the excitation voltage of the UST and the trigger signal are synchronized (from the same FG), an ultrasound pulse is generated and propagates in the data acquisition time window, controlled by acquisition module, after the generation of the FG trigger. Thus, an ultrasound pressure wave as a function of time is acquired at this location. After the completion of the data acquisition, the NI DAQ card sends a digital signal to trigger the translation stage, which is controlled by the software. Then a relatively longer period is used for the hydrophone to be translated to the next location. After that, the digitizer starts waiting for the next trigger signal from the FG to repeat the above steps. Note that the repetition rate of the triggers from the DAQ card (for the translation stage) can be much lower than that of the triggers from the FG, so that multiple times of data acquisitions at each location can be conducted to allow data averaging for improving the signal-to-noise ratio (SNR).

Ultrasonic pressure measurement system II—a fine metal wire-based method:

The system setup (Figure 3) is similar to the hydrophone setup, except the hydrophone is replaced with a small metal wire with a diameter of ~0.46 mm for 1 MHz or a small metal needle with a diameter of ~0.25 mm for higher frequencies (2.25 MHz and 5 MHz). A pulse generator/receiver (5077RP, Olympus NDT, Waltham, Mass, USA) is used to drive the transducer, with a pulse repetition frequency of 200 Hz, energy per pulse of 4 μ joules, a gain of 10 dB, and a low pass filter (20 MHz). The pulse generator/receiver serves both as an ultrasound excitation source and receives and amplifies the reflected ultrasonic echoes from the wire or needle. The received signal is acquired by a digitizer that is triggered by the synchronized output from the pulse generator/receiver. The sequence of data acquisition, triggering, and scanning is similar to the hydrophone system. Compared with the hydrophone system, the data acquired from this system should be processed carefully because the ultrasonic pulses travel a round trip. An example is illustrated in Figures 4 and 5. Figure 4 shows the configuration of the measurement. At each scanning point, we acquire an A-line, which represents an ultrasound echo train. The echoes acquired at any two scanning points along the axial direction (Figure 4) are separated with a distance that is double that of the actual distance because each echo travels a round trip. To remove the effect of the round trip, each scanning point at the first row is used as a reference for all of the other scanning points in the same column (Figure 4). The data acquired from all other points (at the same column) are circularly shifted to the left (Figure 5b) so that

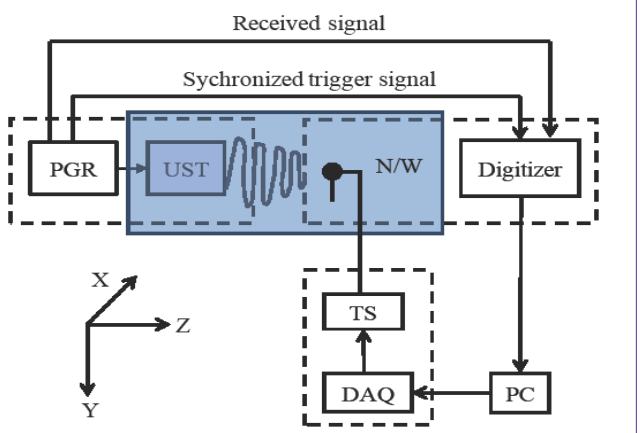

Figure 3: Block diagram of the experimental setup of US propagation using echo from a wire/needle. PGR: Pulse generator/receiver; UST: ultrasound transducer; N/W: needle or metal wire; TS: translation stage; and DAQ: data acquisition card.

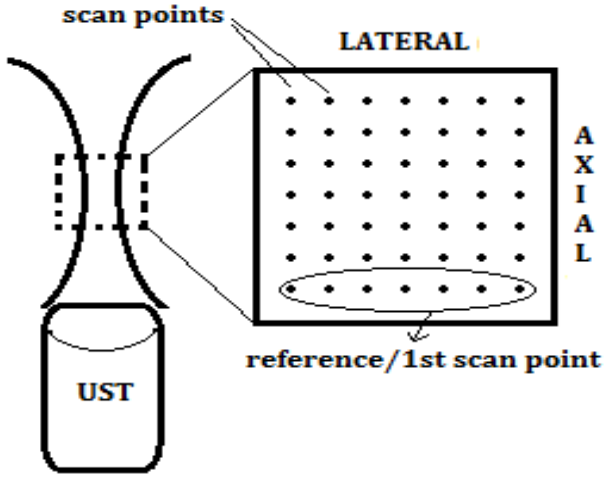

Figure 4: Diagram depicting the area scanned by the hydrophone in the x-z plane.

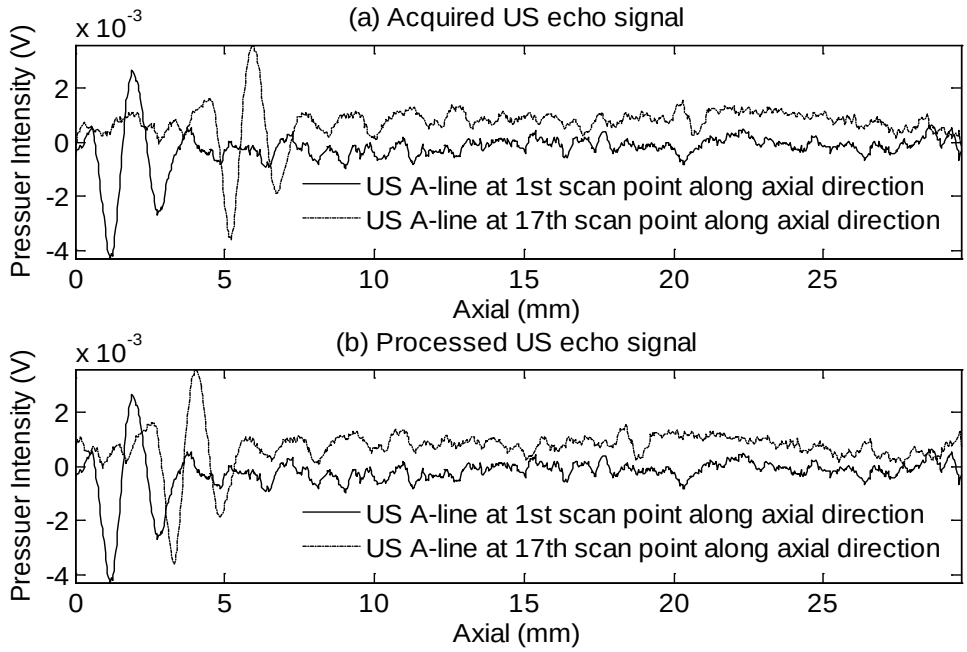

Figure 5: (a) Original US echoes acquired from the pulse generator/receiver. (b) Processed echoes by circularly shifting data points to solve the round trip issue.

the distance measured is equal to the actual distance. Specifically, the number of data points to be shifted in each echo is calculated by the product of the number of the data points acquired per unit distance in water (i.e., the data sampling rate divided by the speed of ultrasound in water) and the axial distance between the scan point in the reference row (first row) and the scan point to be shifted in the subsequent row. As one example, two A-lines are shown in Figure 5a, and they are measured at the scan points of 1st and 17th row along the z (axial) direction and at the 30th column of scanning point along the x (lateral) direction. The distance between the two peaks of the echoes is around 4 mm, which is twice the actual distance of 2 mm. The processed data are shown in Figure 5b, in which the 17th scan point A-line data are circularly shifted toward the left. Now the distance between the two peaks agrees with the actual distance between the two scanning points (~2 mm), thus validating this procedure. The similar processing is done for each column. The rest of data processing is similar to that in the hydrophone system.

Justification of the system cost:

Table 1 lists the major components used in our system, including their features and costs. The function generator with tens of megahertz bandwidth is sufficient for this system, and it is usually available in university undergraduate laboratories. Therefore, the major components for such a system are 3-D translation stage, digitizer, DAQ card, PGR and hydrophone. The total cost of the two systems is ~$13,670.

Software

The entire system is controlled by a custom-made software package developed using MATLAB via a Graphical User Interface (GUI). The software consists of three modules: 3-dimentional position control, data acquisition, and data processing. The 3-dimentional positioning module controls the motion of the hydrophone (or the metal wire or needle), including the initial position, scan range, step size, scan speed, and acceleration. The data acquisition module controls the DAQ card and digitizer, including the sampling rate and time, repetition of scans, delay time between each scanning point, and the data storage. The data processing module controls the reconstruction and display of the ultrasound wave, such as in A-mode and B-mode.

Table 1: The major components used in our systems. The list cost is for guidance only.

Item	Model	Cost
Function generator	AFG 3252, Tektronix	
3D-Translation stage	VXM, Velmex	$3520
Digitizer	USB 5133, National Instrument	$1350
Data acquisition card	PCIe-6353, National Instrument	$1260
Pulse generator and receiver	5073RP, Olympus NDT	$3640
Hydrophone with amplifier	HNP-0200, Onda Corporation	$3900
Metal wires		<$1
Total		$13670

Experiments, Results, and Discussions

Reconstruction of ultrasonic wave propagation using the hydrophone-based system

Figure 6 shows the reconstructed image of the ultrasonic pressure distribution in the x-z plane at the focal area of the UST (V314, Olympus NDT, Center frequency 1MHz) (x: lateral direction and z: axial direction) using the hydrophone-based system. The UST is excited by a 2-cycle sinusoidal burst signal from the FG with a central frequency of 1 MHz and a peak-to-peak voltage of 1 V. Assuming that ultrasound speed in water at 20°C is about 1.48 mm/μs, the wavelength of a 1-MHz ultrasound wave is about 1.48 mm. The image shown in Figure 6 represents a snapshot of the ultrasonic wave propagation around the focal zone of the UST. The gray scale represents variation in the acoustic pressure. White and black represent positive and negative pressure, respectively. The wavelength can be estimated as about 1.5 mm from the two adjacent positive peaks, which is close to the literature value of 1.48 mm [1]. The corresponding video (online) in Figure 6 shows the dynamic propagation of the reconstructed ultrasound pressure wave in the UST focal zone. These results show that the hydrophone-based system can accurately reconstruct the dynamic ultrasonic pressure distribution.

Advantages of using a hydrophone are as follows: (1) it can measure the absolute value of the ultrasonic pressure provided the hydrophone is calibrated; (2) compared with the wire-based method, the data processing is relatively simple; (3) it does not require a pulse generator/receiver, which is usually a little more expensive than a needle hydrophone; and (4) due to the high sensitivity of the hydrophone (in micron Pascal range), it is not necessary to amplify the driving signal with a radio frequency (RF) amplifier, which is usually expensive. The disadvantage is that the lateral spatial resolution of the reconstructed image is limited by the physical diameter of the hydrophone tip (the axial resolution is related to the system dynamic response speed and is not limited by the physical size of the hydrophone). In this study, the hydrophone diameter is about 200 microns, which is sufficient for the reconstruction of focused pressure waves at a low frequency, such as 1-5 MHz, or unfocused ultrasound waves. Note that the measured ultrasound pressure wave represents the convolution between the excitation voltage signal and the impulse response functions of the UST, the hydrophone, and its amplifier. Therefore, the bandwidth of the measured signal is determined by the one that has the narrowest bandwidth, which is the UST.

Reconstruction of ultrasonic wave propagation using the wire-based system

Figure 7 shows the reconstructed image of the ultrasonic pressure distribution in the x-z plane at the focal area of the 1 MHz UST (x: lateral direction and z: axial direction) using the wire-based system. The pulse generator/receiver sends a narrow and negative high-voltage pulse to excite the UST. Thus, a narrow ultrasonic pulse is generated and propagates in the water. When the pulse reaches the small metal wire, it is partially reflected and detected by the same UST and the pulse generator/receiver. Therefore, the measured signal represents the convolution between the excitation voltage pulse and the impulse response functions of the UST, the wire reflection, the same UST, and the receiver amplifier. The same as with the hydrophone system, the signal bandwidth is determined by the UST's bandwidth. Similar to the hydrophone experiment, the image shown in Figure 7 represents a snapshot of the ultrasonic wave propagation around the focal zone of the UST. The gray scale of the image represents the distribution of the ultrasound pressure field in the focal zone in water. The pressure wave approximately has one sinusoidal cycle of a 1-MHz wave. The white and black show the positive and negative pressure, respectively. This is because that the excitation voltage signal is a very narrow electronic pulse, and the UST has a central frequency of 1 MHz with a limited bandwidth (~50% of the central frequency). The wavelength observed from the distance between the two negative peaks along the axial direction is about 1.53 mm, which is close to the value measured using the hydrophone system. The corresponding video (online) in Figure 7 shows the dynamic propagation of the reconstructed ultrasound pressure wave in the UST focal zone. These results show that the wire-based system can also accurately reconstruct the dynamic ultrasonic pressure distribution. Note that the results in Figure 7 have much better SNR than those measured

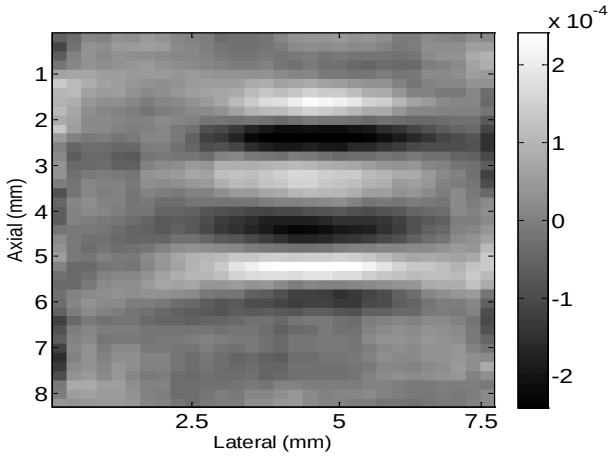

Figure 6: A snapshot of the reconstructed 2-D (x-z or lateral-and-axial) image of the pressure distribution of an ultrasound pulse at the focal zone generated from a 1 MHz UST and measured using the hydrophone-based system. The corresponding online video shows the propagation of the reconstructed ultrasound pressure wave in the UST focal zone using the hydrophone-based system (enhanced online).

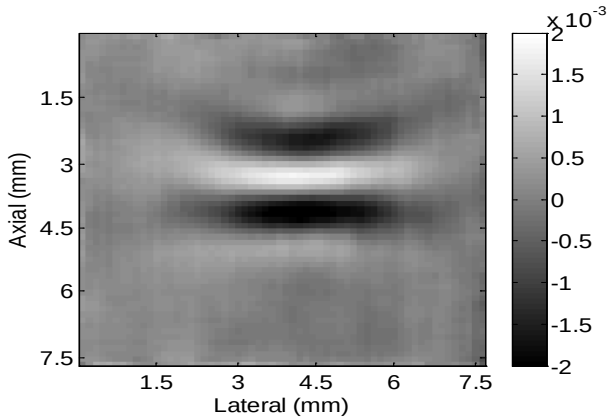

Figure 7: A snapshot of the reconstructed 2-D (x-z or lateral-and-axial) image of the pressure distribution of an ultrasound pulse at the focal zone generated from a 1 MHz UST and measured using the wire-based system. The diameter of the metal wire is 0.46 mm. The corresponding online video shows the propagation of the reconstructed ultrasound pressure wave in the UST focal zone using the wire-based system (enhanced online).

by the hydrophone-based system in Figure 6. This is mainly because the voltage applied across the UST in the wire-based system is much higher (~-120 V) than that in the hydrophone-based system (1 V, for avoiding potential damage to the hydrophone).

Similar experiments were carried out using a 2.25 MHz (V305, Olympus NDT) and a 5 MHz (V308, Olympus NDT) UST and a small needle with a diameter of 0.25 mm. The results of the corresponding snapshots and videos (online) are shown in Figures 8 and 9, respectively. Note that, because the focal zone is significantly reduced when increasing the ultrasound frequency, the scanning areas are correspondingly reduced from 7.62 x 7.62 mm^2 for 1 MHz UST to 2.54 x 5 mm^2 and 3.81 x 2.54 mm^2 for 2.25 and 5 MHz USTs, respectively. The ultrasound wavelength (along the axial direction) is about 0.61 mm and 0.38 mm for 2.25 and 5 MHz, respectively, which agrees with the calculated values of 0.66 and 0.29 mm, respectively, when assuming that the ultrasound speed is 1.48 mm/μs in 20°C water. A large error occurs for 5 MHz UST. This is because the focal volume becomes smaller when the frequency increases.

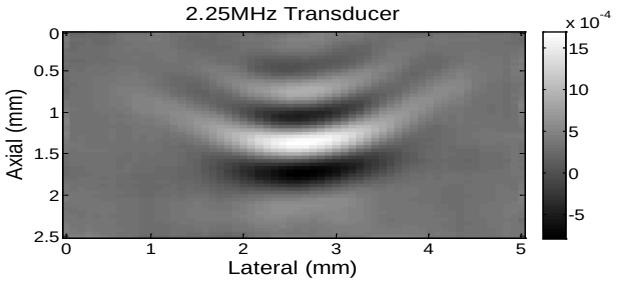

Figure 8: A snapshot of the reconstructed 2-D (x-z or lateral-and-axial) image of the pressure distribution of an ultrasound pulse at the focal zone generated from a 2.25 MHz UST and measured using a metal wire of diameter 0.25 mm. The corresponding online video shows thepropagation of the reconstructed ultrasound pressure wave in the UST focal zone (enhanced online).

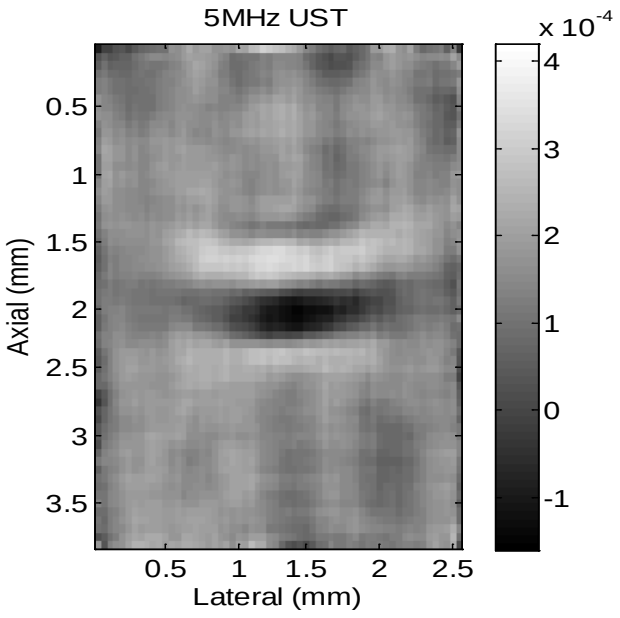

Figure 9: A snapshot of the reconstructed 2-D (x-z or lateral-and-axial) image of the pressure distribution of an ultrasound pulse at the focal zone generated from a 5 MHz UST and measured using a metal wire of diameter 0.25 mm. The corresponding online video shows thepropagation of the reconstructed ultrasound pressure wave in the UST focal zone (enhanced online).

The advantages of using the wire-based setup are: (1) no hydrophone is needed, which is valuable because a needle hydrophone is usually vulnerable when exposed to ultrasound pressure for a long time; (2) a small-diameter metal wire is usually available; and (3) the lateral spatial resolution may be improved by reducing the diameter of the wire, which is much easier to achieve and less expensive than reducing the hydrophone diameter. The disadvantages are that: (1) a pulse generator/receiver is needed, which is expensive if a commercial one is adopted, such as the one used in this study (~$3,500), though a homemade pulse generator/receiver may be much cheaper than a commercial one by reducing unnecessary features; (2) when processing the data, the round trip traveling of the sound has to be considered; and (3) because the ultrasound pulse is generated and detected by the same UST, the actual ultrasound wave is convolved with the impulse response function of the UST twice compared to once in case of the hydrophone system. Because the UST usually has a much narrower bandwidth than the hydrophone, the second convolution of the ultrasound pressure with the impulse function of the UST may more significantly distort the actual ultrasound pressure than the convolution of the ultrasound pressure with the impulse response function of the hydrophone. However, this problem can be overcome if one can de-convolve the measured signal from the response function of the UST or hydrophone.

Reconstruction of ultrasonic wave interference using the hydrophone-based system

The interference between two ultrasonic waves is an important phenomenon, and to reconstruct efficiently the dynamics of ultrasound interference is one of the goals of this study. We adopted the hydrophone-based experimental system. In the setup, two synchronized output channels from the FG were used to drive simultaneously two 2.25 MHz unfocused UST (Olympus Pan metrics A306S-SU). The two USTs were arranged perpendicular to each other. The USTs were pulsed at 2.25 MHz with 1 cycle per pulse, with a peak-to-peak voltage of 1.8 V. The hydrophone was positioned at the intersection of the two ultrasonic waves with the same relative distances from the two USTs. Similarly, the dynamic ultrasound pressure distribution can be reconstructed by scanning the hydrophone in an area of interest that is 2.5 x 2.5 mm^2. Figure 10a shows a snapshot and the dynamic propagation (online) of the reconstructed interfered pressure field. Clearly, the two waves are interfered at the common area (Figure 10a), where a small negative pressure region (surrounded by a few positive pressure areas) is formed. As the two waves are propagating toward their own directions

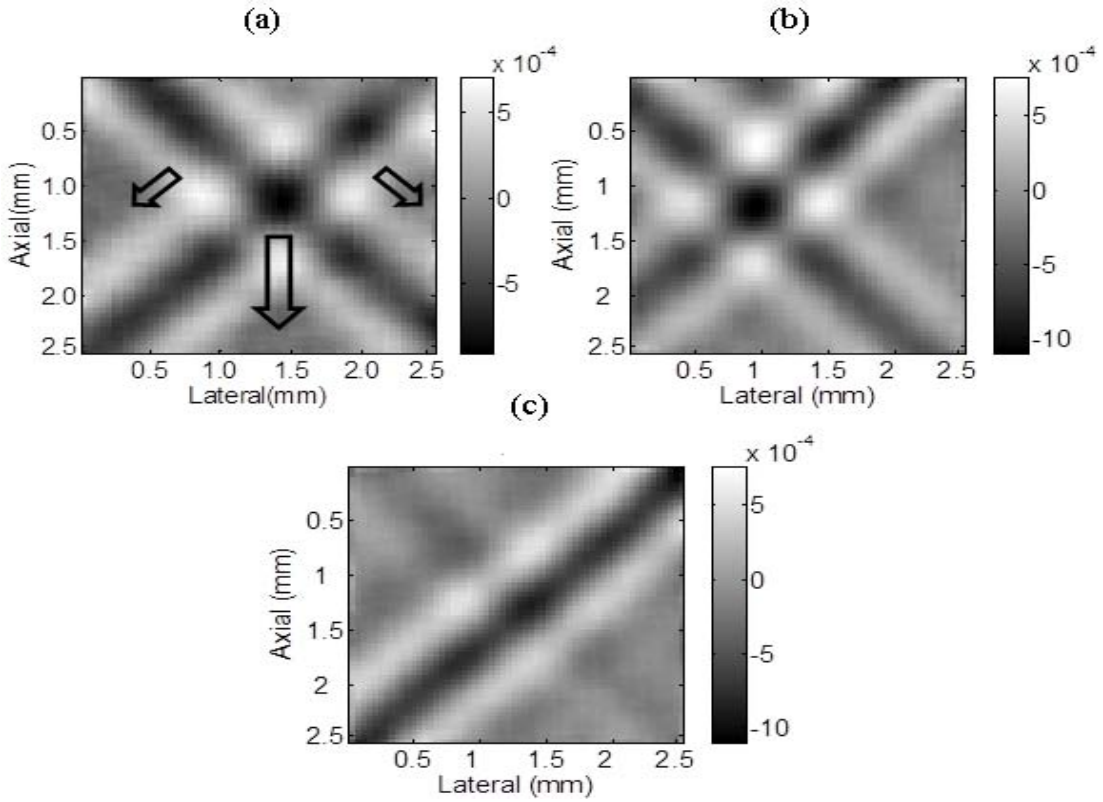

Figure 10 : A snapshot of the reconstructed interference between two ultrasound pressure waves at 2.25 MHz: (a) with no chicken tissue; (b) with a piece of chicken breast tissue (12 mm in thickness) in front of the right transducer; and (c) with a piece of chicken breast tissue (24 mm in thickness) in front of right transducer. The corresponding online videos show the propagations of these interfered waves (enhanced online).

(see the two small arrows), the interfered pressure area travels along the diagonal direction (see the large arrow) of the two directions.

To investigate the effect of tissue heterogeneity on the interference field, a piece of chicken breast tissue was added in front of one of the ultrasound transducers. Figure 10b (along with its online video) and Figure 10c (along with its online video), respectively, show the results when a piece of chicken breast tissue with a thickness of 12 and 24 mm is placed in front of one of the transducers. Clearly, it can be seen that the chicken breast tissue has very little effect on the patterns of the ultrasound pressure waves and their interference. When the thickness is increased to 24 mm, the ultrasound amplitude is significantly reduced due to the tissue absorption and reflection. However, the patterns of the waves and their interference are less affected. This is understandable because acoustic waves usually are much less scattered by biological soft tissue compared with optical waves.

Ultrasound imaging using a single ultrasound transducer

Another application of the system is to conduct ultrasound imaging. Simply by replacing the wire with a plastic tube and scanning with the focused ultrasound transducer, the cross-section of the tube can be ultrasonically imaged. Figure 11 shows an experimental setup. Briefly, a water- or micro bubble solution-filled plastic tube was submerged into a water tank. A 5 MHz focused UST (V308, Olympus Pan metrics) was laterally scanned along the x direction. The tube

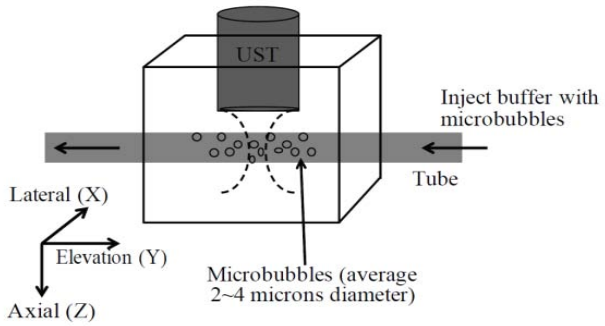

Figure 11 : Experimental setup for ultrasound imaging of a small tube (outer diameter = 2.39 mm, inner diameter = 0.79 mm) filled with different concentrations of micro bubbles.

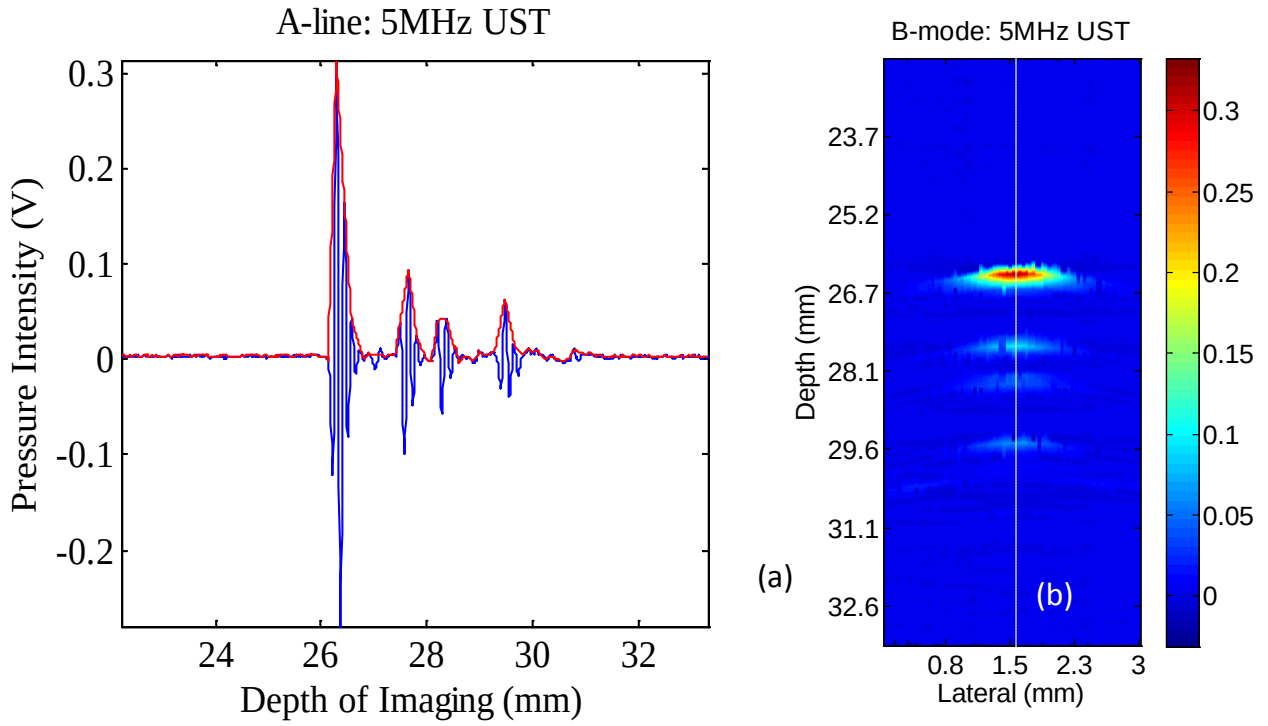

Figure 12 : (a) An A-line of raw ultrasound signal and it's envelop (recorded along the white dotted line shown in (b)) when the tube is filled with water. (b) A B-mode ultrasound image of the cross-section of the tube form by displaying multiple envelopes of the A-lines in (a), which were acquired by scanning the ultrasound transducer laterally.

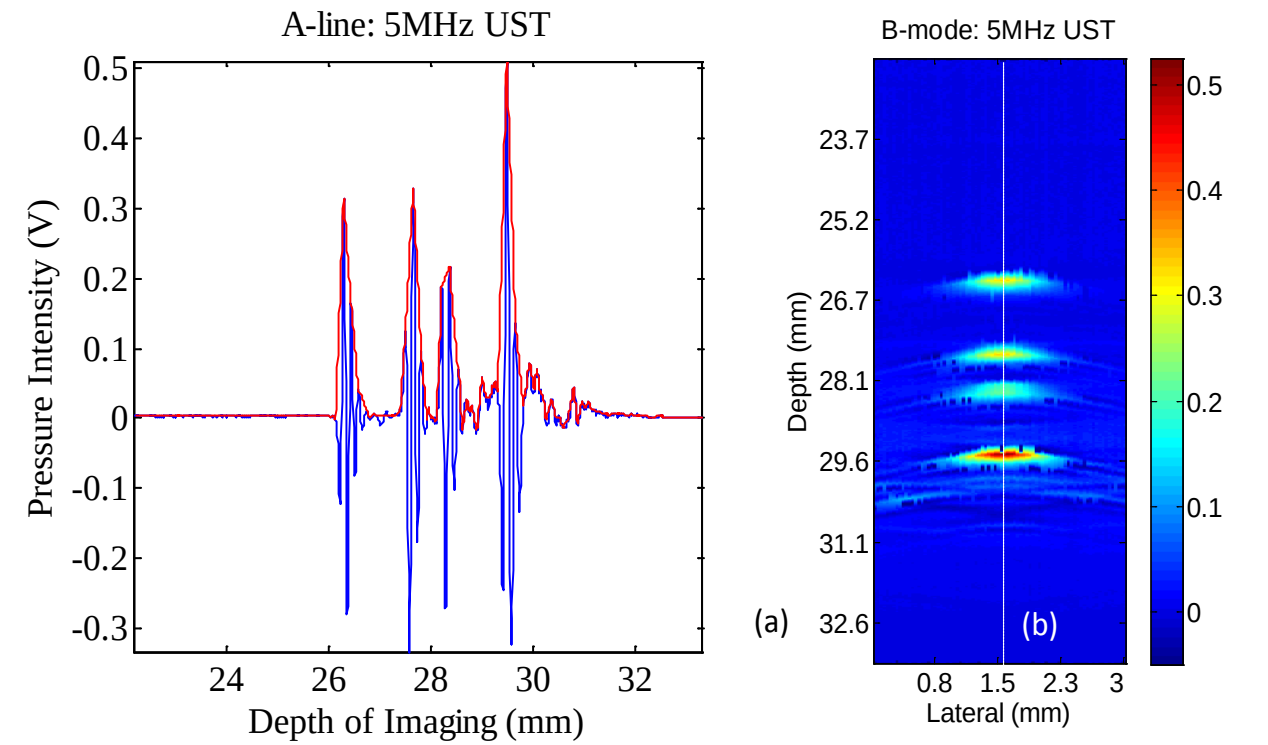

Figure 13 : The compensated results of Figure 12(a) A-line and (b) B-mode image.

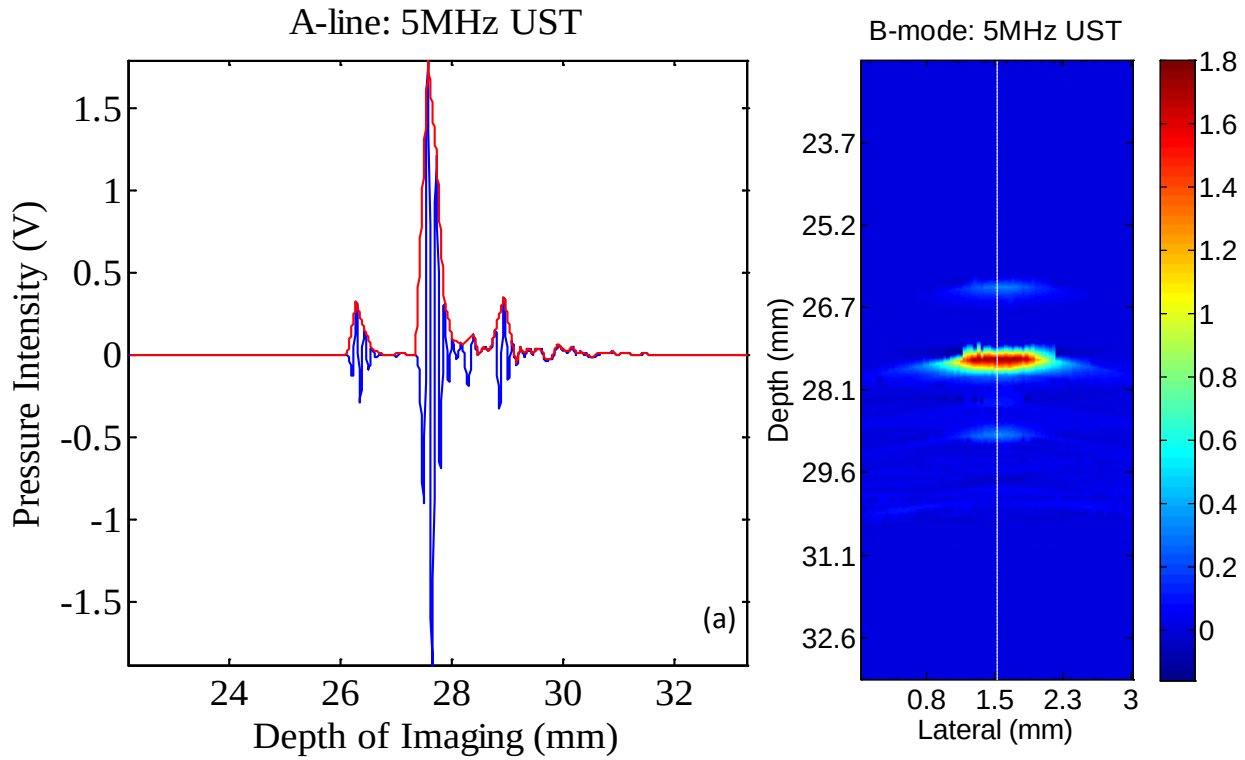

Figure 14 : (a) An A-line of a raw ultrasound signal and its envelope (recorded along the white dotted line shown in (b)) when the tube is filled with air. (b) The corresponding B-mode ultrasound image of the cross-section of the tube.

is positioned at the UST focal zone, achieving an optimized lateral resolution. Figure 12 shows the acquired RF raw data from a water-filled tube. Figure 12a represents a RF A-line along the white dotted line indicated in Figure 12b. When scanning the transducer laterally, multiple A-lines were acquired, and their envelopes (as represented by the red curve over the blue one in Figure 12a) were displayed in Figure 12b to form a B-mode image. Thus, the cross-section of the tube can be visualized from top to bottom in the Figure 12b. Clearly, four boundaries of tube were resolved. The top (closest to UST) and bottom (farthest from UST) in Figure 12b represent the outer boundaries, and the two lines in the middle represent the inner boundaries of the tube. Due to the attenuation of the ultrasound energy when the pulse propagates from the top to the bottom, reflected peaks from the boundary are usually attenuated exponentially. To compensate for this attenuation, the RF raw data are multiplied by a gain factor that is exponentially increasing as a function of the depth. Figure 13 shows the compensated results. From this Figure 13, the outer and inner diameters of the tube were calculated to be around 0.9 mm and 3 mm, respectively, which is close to the actual inner (0.79 mm) and outer (2.39 mm) diameter of the tube. Also, it can be seen that the lateral resolution of the image is lower than the axial resolution due to the finite lateral size of the focal zone of the UST.

After draining the water from the tube with the air left inside, the ultrasound image is shown in Figure 14. Clearly, the majority of the ultrasound energy is reflected at the tube and air boundary (see the peak of the A-line in Figure 14a and the bright line in Figure 14b). An ultrasound shadow is formed below the air layer, which overwhelms the echo from the third and fourth boundaries making them very weak or invisible, as shown in Figure 14b. Micro bubbles have been used as ultrasound imaging contrast agents for many years [9]. Figure 15 shows the results when injecting a high concentration of approximately 9% micro bubbles (by mixing 0.02 ml 99.8% micro bubble solution to 0.2 ml buffer solution), which is about 1.8 x 10^8 particles/ml. (Targestar-SA, Targeson, Inc., mean diameter 2.36 ± 0.03 μm.) The image is similar to the one acquired from the tube filled with air. This is mainly due to the highly concentrated micro bubbles, which reflect a large amount of ultrasound energy. When decreasing the micro bubble concentration to approximately 2.5% (by mixing 0.02 ml 99.8% micro bubble solution with a 0.6 ml buffer solution), which is about 0.58 x 10^8 particles/ml, the reflected signal from the micro bubbles becomes weak (Figure 16). Thus, all four of the boundaries are visible again. More importantly, a small signal peak can be observed between the 2nd and 3rd boundaries (Figure 16a), which is due to the reflection of the micro bubbles. Correspondingly, a small hot spot occurs right below the 2nd boundary (Figure 16b), which is due to the reflection of the micro bubbles. Note that Figures 12b and 13b do not show this type of signal where water is filled in the tube (no micro bubbles). Because micro bubbles are filled with gas, the density is much lower than that of the surrounding liquid. Therefore, most micro bubbles are accumulated on the top of the tube.

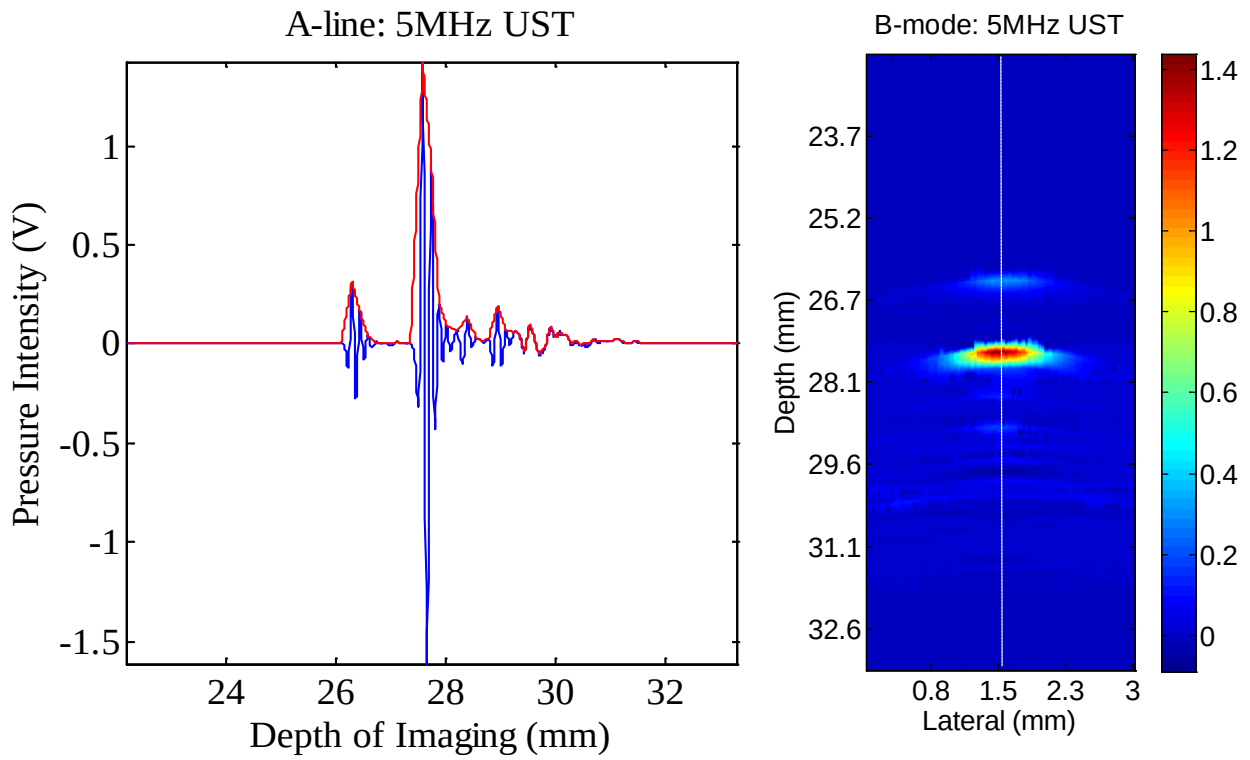

Figure 15 : (a) An A-line of a raw ultrasound signal and its envelope (recorded along the white dotted line shown in (b)) when the tube is filled with a high concentration of the microbubble solution (~9%). (b) The corresponding B-mode ultrasound image of the cross-section of the tube when filled with the high-concentration microbubble solution.

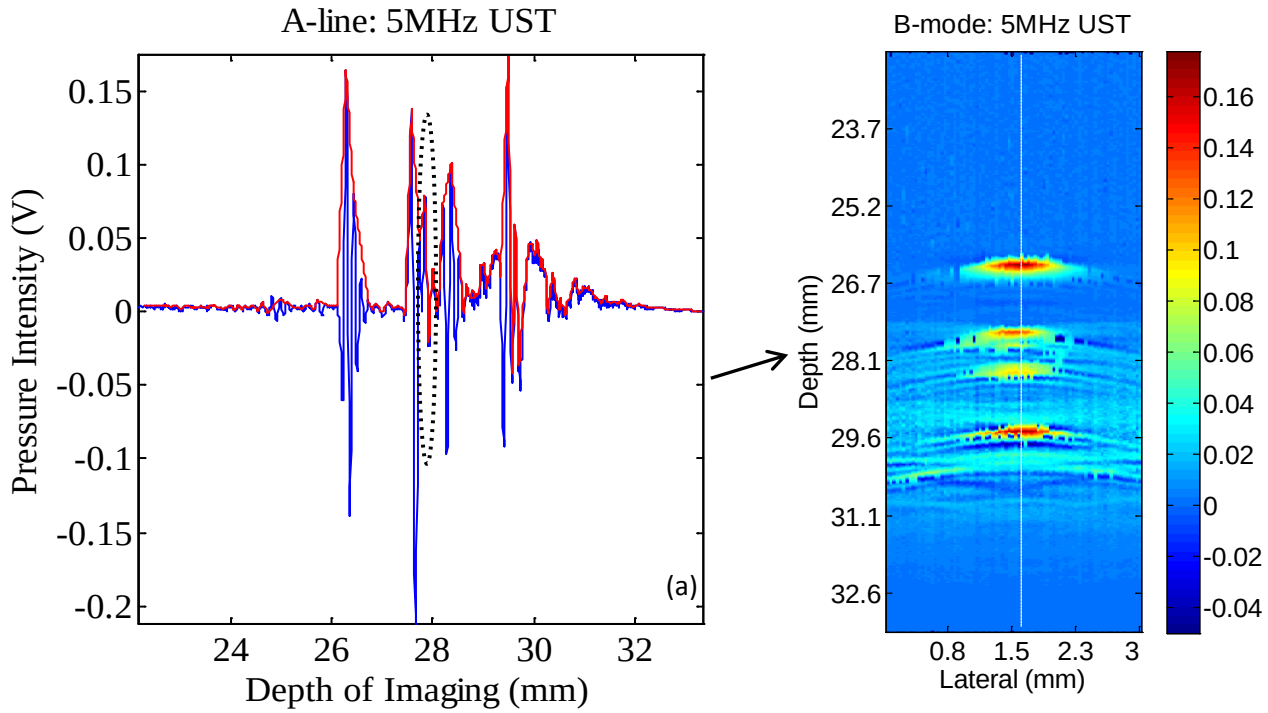

Figure 16 : (a) An A-line of a raw ultrasound signal and its envelope (recorded along the white dotted line shown in (b)) when the tube is filled with a low concentration of microbubble solution (~2.5%). (b) The corresponding B-mode ultrasound image of the cross-section of the tube when filled with the low-concentration microbubble solution.

Conclusion

Two relatively simple and cost-efficient systems have been demonstrated for 2-dimentional imaging of ultrasound pressure wave propagation in water. Both the hydrophone approach (direct measurement of ultrasound pressure wave) and the wire/needle approach (pulse and echo) have been shown to be useful in reconstructing the ultrasound pressure waves and proved efficient in demonstrating ultrasound wave propagation and its characteristics (to various group of students) as part of 'Tissue Ultrasound-optical imaging lab' course curriculum at University of Texas at Arlington with a positive feedback. The reconstruction of ultrasound interference between two unfocused ultrasound pulses has also been successfully demonstrated. Ultrasound imaging and micro bubble-enhanced ultrasound imaging were also presented. Therefore, the presented systems are useful tools for visualizing the propagation and interference of ultrasound pressure waves and for understanding ultrasound imaging principles with a limited budget.

Acknowledgment

This work was supported in part by funding from the NIH/NIBIB 7R15EB012312-02 (Yuan), the CPRIT RP120052 (Yuan) and the NSF CBET-1253199 (Yuan).

References

1. Szabo TL. Diagnostic ultrasound imaging: Inside Out. Massachusetts: Elsevier Academic Press. 2004.
2. Raum K, O'Brien WD. Pulse-Echo field distribution measurement technique for high-frequency ultrasound sources. IEEE Trans Ultrason Ferroelectr Freq Control. 1997; 44: 810-815.
3. Passmann C, Ermert H. A 100-MHz ultrasound imaging system for dermatologic and ophthalmologic diagnostics. IEEE Trans Ultrason Ferroelectr Freq Control. 1996; 43: 545-552.
4. Foster FS, Pavlin CJ, Harasiewicz KA, Christopher DA, Turnbull DH. Advances in ultrasound biomicroscopy. Ultrasound Med Biol. 2000; 26: 1-27.
5. Schutt EG, Klein DH, Mattrey RM, Riess JG. Injectable microbubbles as contrast agents for diagnostic ultrasound imaging: the key role of perfluorochemicals. Angew Chem Int Ed Engl. 2003; 42: 3218-3235.
6. Morgan KE, Allen JS, Dayton PA, Chomas JE, Klibaov AL, Ferrara KW. Experimental and theoretical evaluation of microbubble behavior: effect of transmitted phase and bubble size. IEEE Trans Ultrason Ferroelectr Freq Control. 2000; 47: 1494-1509.
7. Kiessling F, Huppert J, Palmowski M. Functional and molecular ultrasound imaging: concepts and contrast agents. Curr Med Chem. 2009; 16: 627-642.
8. Ferrara K, Pollard R, Borden M. Ultrasound microbubble contrast agents: fundamentals and application to gene and drug delivery. Annu Rev Biomed Eng. 2007; 9: 415-447.
9. Blomley MJ, Cooke JC, Unger EC, Monaghan MJ, Cosgrove DO. Microbubble contrast agents: a new era in ultrasound. BMJ. 2001; 322: 1222-1225.
10. Charlebois TF, Pelton RC. Quantitative 2D and 3D Schlieren Imaging for acoustic power and intensity measurements. Medical Electronics. 1995; 66-73.
11. Huang B, Shung KK. Characterization of high-frequency, single-element focused transducers with wire target and hydrophone. IEEE Trans Ultrason Ferroelectr Freq Control. 2005; 52: 1608-1612.
12. Huang B, Shung KK. Characterization of very high frequency transducers with wire target and hydrophone. IEEE Trans Ultrason Ferroelectr Freq Control. 2005; 52: 1608-1612.
13. OptiSon® Ultrasound Beam Analyzer.
14. Acoustic Intensity Measurement System.

Austin J Biomed Eng - Volume 1 Issue 1 - 2014
ISSN : 2381-9081 | www.austinpublishinggroup.org

Citation: Kandukuri J, Liu Y , Yuan B. Cost-Efficient and Multi-Functional Systems for Ultrasound Measurement and Imaging. Austin J Biomed Eng. 2014;1(1): 1001.